A shape optimization approach towards improving the understanding of magmatic plumbing system

Théo Perrot[1], Freysteinn Sigmundsson[2], Charles Dapogny[3]

[1]Mechanical engineering department, Ecole Normale Supérieure Paris-Saclay
[2]Institute of Earth Sciences, University of Iceland
[3]Jean Kuntzmann Institute, CNRS, Grenoble-Alpes University

Key Points:

- We present a novel approach to allow for assessment of volcanic magma domains shape based on level-set shape optimization.
- It relies on numerical finite element models iteratively modified to minimize the discrepancy to observed surface displacements
- We found strong dependence of best solution to initialization when benchmarked with synthetic data but application on data from Svartsengi 2022 inflation outputed relevant results.

Corresponding author: Théo Perrot, `theo.perrot@ens-paris-saclay.fr`

Abstract

In volcano geodesy, pressure sources in volcano roots responsible for surface movements are inverted using ground deformation data after defining a forward parametric model for the source. Such models are most of the time relying on predefined shape for the source, which can limit their accuracy. On the contrary, we propose here a shape optimization method to invert for pressure sources without any prior shape assumption. With that flexibility, the optimal shape of a pressurized magma body is determined by minimizing the discrepancy between observed and modelled displacement. We explore the capabilities of this approach with synthetic data first for validation and then apply it to observed ground deformation at the Svartsengi volcanic system in Iceland, demonstrating its potential to improve volcanic hazard assessment after maturation with further work.

Plain Language Summary

Reservoirs beneath volcanoes contain pressurized magma that can feed eruptions when it breaks through. Because the pressure on the surrounding rocks is so high, the reservoir causes changes in ground motion at the surface that can be detected by instruments. Geophysicists use these measurements to reconstruct the position, orientation, and pressure of reservoirs in the crust and to determine the likelihood of a future eruption. Here we present a new method that could allow them to also reconstruct the shape of these reservoirs, which are often odd and irregular, while current reconstruction methods assume nice and smooth shapes such as spheres. This method is based on shape optimization, a framework widely used in fields such as engineering, where it is used to improve the design of objects or mechanisms. We tested the method on synthetic motion data and on real data from the Svartsengi volcanic system in Iceland. Although our results show that the method needs to be improved before it can be used in operational monitoring, they pave the way for future developments and may help to better reconstruct magma reservoirs.

^{TP}: [https://www.agu.org/Share-and-Advocate/Share/Community/Plain-language-summary]

1 Introduction

^{TP}: [Section ok]

In volcano geodesy, inverse problems are central to estimating the position of pressurized magma bodies at depth in volcano roots, using observed crustal deformation as a proxy. The displacement is measured by e.g. Global Navigation Satellite System (GNSS) point positioning, leveling campaigns, or interferometry analysis of synthetic aperture radar (InSAR) in a volcanic region (Dzurisin, 2007). The subsurface processes causing the movement are inferred from these observations. Magmatic sources are modeled as pressurized cavities that deform the surrounding host rocks and cause the surface to move. Various inversion methods based on parametric analytical or numerical models aim at finding the optimal values for the vector of d free parameters $\underline{m} \in \mathbb{R}^d$ of a model. An error function $J(\underline{m})$ is representative of the misfit between the observed displacements and the prediction of the model. $\underline{m}_{opt}$ can then be found using various inversion techniques minimizing J: global optimization based on analytic (Cervelli et al., 2001) or numerical models (Hickey & Gottsmann, 2014; Charco & Galán del Sastre, 2014), Bayesian inference (Bagnardi & Hooper, 2018; Trasatti, 2022), or genetic algorithms (Velez et al., 2011) on analytic models. The choice of the method can be influenced by what is feasible regarding the number of evaluations of $J(\underline{m})$: numerical models handle a complex description of the system, but are computationally expensive compared to analytic models, which on the other hand rely on strong simplifying assumptions (Taylor et al., 2021).

However, each of these finite-dimensional optimization methods is limited by the intrinsic assumption of a definite parametric shape for the source. In fact, analytic expressions can be derived for only a few regular shapes such as point source (Mogi, 1958), finite sphere source (McTigue, 1987), or ellipsoidal source (Yang et al., 1988), and any numerically generated shape must be parameterized to be inverted. A workaround would be an approach relying on shapes parameterized with more parameters, such as B-splines surfaces, to allow more exploration in the possible shapes. *TP:*This implies optimization within a high-dimension domain, bringing unpleasant phenomena known as the curse of dimensionality [Ref needed]. The goal of this paper is not to give a definitive answer to these limitations, but rather to lay the first stone for a new approach that overcomes these difficulties.

1.1 Shape optimization

Shape optimization generally aims to minimize a cost function depending on the domain. This practice is very popular in various disciplines, such as structural mechanics, where one typically wishes to improve the stiffness of a solid structure (Bendsoe & Sigmund, 2004), fluid mechanics, where it is applied to the design of pipes, heat exchangers or flying obstacles (Feppon, Allaire, Dapogny, & Jolivet, 2020), or again electromagnetism (Lucchini et al., 2022). Beyond academic investigations, it has aroused a tremendous enthusiasm in industry; nowadays, most Finite Element simulation and design softwares include a shape optimization module (Frei, 2015), (Slavov & Konsulova-Bakalova, 2019), (Le Quilliec, 2014). However, the use of these techniques in volcano geodesy is new to the best of our knowledge.

Multiple shape and topology optimization frameworks are available, see e.g. the review in (Sigmund & Maute, 2013). One popular strategy describes the design as a density function ρ on a large, fixed computational domain: ρ takes values 0 and 1 in the void and material regions, respectively, and intermediate values in between account for a fictitious mixture of both (Sigmund, 2001; Bendsoe & Sigmund, 2004). One major drawback of this approach is that it does not feature a clear representation of the boundary of the optimized design; in particular, approximations are needed to calculate physical quantities related to the domain at play. To alleviate this issue, we rely on a recent version of the Level Set method for shape optimization, which benefits from an explicit representation of the boundary at each step of the optimization.

2 Method

This section describes the considered shape optimization problem and its practical implementation. For a more complete mathematical background, we refer to e.g. (Allaire et al., 2021).

2.1 Presentation of the physical model

The region under scrutiny is represented by a fixed bounded domain $D \subset \mathbb{R}^3$, which is made of two complementary subdomains Ω and $\Omega^c := D \setminus \overline{\Omega}$, where:

- The cavity $\Omega \Subset D$ stands for the magma chamber, whose shape is to be reconstructed. Its boundary $\Gamma = \partial\Omega$ is subjected to the force $\mathbf{f} = \Delta P \mathbf{n}$, aligned with the unit normal vector $\mathbf{n} : \Gamma \to \mathbb{R}^3$ to Γ pointing outward Ω, and whose magnitude equals the (given) pressure difference ΔP between the cavity and the surrounding crust, see Section 4 for a discussion about this point.
- The complement Ω^c of Ω represents the surrounding Earth crust. It is filled by a homogeneous, isotropic elastic material. The displacement of the bottom side Γ_b of ∂D is set to $\mathbf{0}$ and the other boundary regions of D are free of stress.

This setting is illustrated on Fig. 1 (a). The displacement $\mathbf{u}_\Omega : \Omega^c \to \mathbb{R}^3$ of the crust in these circumstances is the solution to the system of linearized elasticity:

$$\begin{cases} -\mathrm{div}(Ae(\mathbf{u}_\Omega)) = \mathbf{0} & \text{in } \Omega^c, \\ \mathbf{u}_\Omega = \mathbf{0} & \text{on } \Gamma_{\mathrm{b}}, \\ Ae(\mathbf{u}_\Omega)(-\mathbf{n}) = \mathbf{f} & \text{on } \Gamma, \\ Ae(\mathbf{u}_\Omega)\mathbf{n} = \mathbf{0} & \text{on } \partial D \setminus \overline{\Gamma_{\mathrm{b}}}, \end{cases} \tag{1}$$

where $e(\mathbf{u}) := \frac{1}{2}(\nabla \mathbf{u} + \nabla \mathbf{u}^T)$ is the strain tensor induced by a displacement $\mathbf{u}$ and A is the Hooke's law of the crust material.

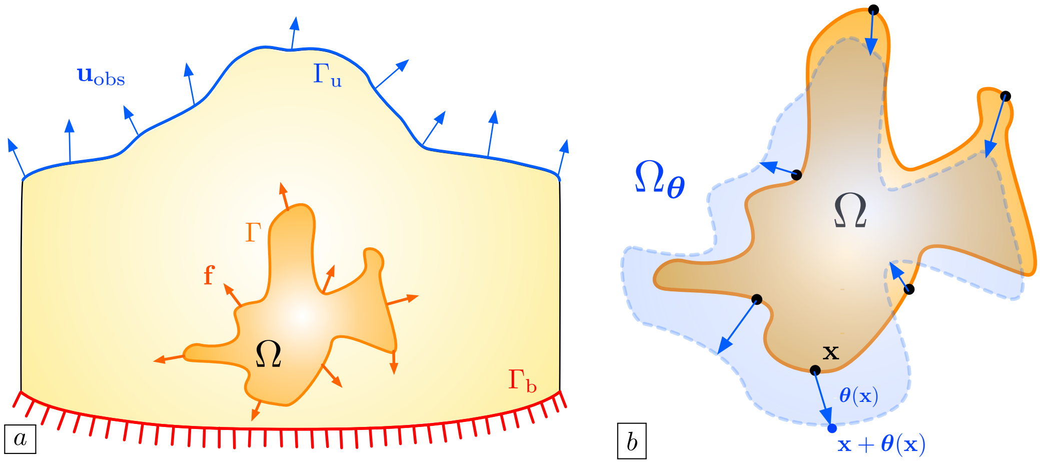

Figure 1. *(a) Sketch of the physical model; (b) Variation $\Omega_{\boldsymbol{\theta}}$ of Ω.*

2.2 Shape optimization for the reconstruction of the magma chamber

In the applications of this article, the shape Ω of the magma chamber is unknown. From the datum of observed values $\mathbf{u}_{\mathrm{obs}} : \Gamma_{\mathrm{u}} \to \mathbb{R}^3$ of the displacement of the crust on the upper surface Γ_{u} of D, we intend to identify Ω as the solution to the following shape optimization problem:

$$\min_{\Omega \subset D} J_{\mathrm{LS}}(\Omega), \text{ where } J_{\mathrm{LS}}(\Omega) := \int_{\Gamma_{\mathrm{u}}} |\mathbf{u}_\Omega - \mathbf{u}_{\mathrm{obs}}|^2 \, \mathrm{d}s, \tag{2}$$

featuring the least-square discrepancy between the prediction $\mathbf{u}_\Omega$ of the physical model (1), and the observed displacement $\mathbf{u}_{\mathrm{obs}}$ on Γ_u.

2.3 Shape derivatives

The treatment of (2) calls for a notion of derivative for a function $J(\Omega)$ of the domain Ω. In this work, we rely on the boundary variation method of Hadamard, see (Allaire, 2006; Allaire et al., 2021; Henrot & Pierre, 2018; Murat & Simon, 1976). In short, variations of a reference domain Ω are considered under the form

$$\Omega_{\boldsymbol{\theta}} := (\mathrm{Id} + \boldsymbol{\theta})(\Omega), \text{ where } \boldsymbol{\theta} : \mathbb{R}^3 \to \mathbb{R}^3 \text{ is a “small” vector field,}$$

see Fig. 1 (b). The shape derivative $J'(\Omega)(\boldsymbol{\theta})$ of a function $J(\Omega)$ at Ω is the derivative of the underlying mapping $\boldsymbol{\theta} \mapsto J(\Omega_{\boldsymbol{\theta}})$, which produces the following expansion:

$$J(\Omega_{\boldsymbol{\theta}}) = J(\Omega) + J'(\Omega)(\boldsymbol{\theta}) + \mathrm{o}(\boldsymbol{\theta}), \text{ where } \frac{\mathrm{o}(\boldsymbol{\theta})}{||\boldsymbol{\theta}||} \xrightarrow{\boldsymbol{\theta} \to \mathbf{0}} 0. \tag{3}$$

In practice, $J'(\Omega)(\boldsymbol{\theta})$ is used to identify a descent direction $\boldsymbol{\theta}$, i.e. a vector field such that

$$J'(\Omega)(\boldsymbol{\theta}) < 0, \text{ so that for a ``small'' step } \tau > 0, \quad J(\Omega_{\tau\boldsymbol{\theta}}) \approx J(\Omega) + J'(\Omega)(\boldsymbol{\theta}) < J(\Omega).$$

Intuitively, the perturbed shape $\Omega_{\tau\boldsymbol{\theta}}$ performs "better" than Ω with respect to $J(\Omega)$.

The calculation of the shape derivative of the functional $J_{\text{LS}}(\Omega)$ in (2) is a tedious, but classical issue. It can be realized thanks to the adjoint method, see e.g. (Cea, 1986; Plessix, 2006) and (Allaire et al., 2004) in this particular mathematical context:

$$J'_{\text{LS}}(\Omega)(\boldsymbol{\theta}) = \int_\Gamma v_\Omega \, (\boldsymbol{\theta}\cdot\mathbf{n}) \, \mathrm{d}s, \text{ where } v_\Omega := -Ae(\mathbf{u}_\Omega) : e(\mathbf{p}_\Omega) - \Delta P \, \mathrm{div}(\mathbf{p}_\Omega), \tag{4}$$

and the adjoint state $\mathbf{p}_\Omega$ is the solution to the following problem:

$$\left\{ \begin{array}{cl} -\mathrm{div}(Ae(\mathbf{p}_\Omega)) = \mathbf{0} & \text{in } \Omega^c, \\ \mathbf{p}_\Omega = \mathbf{0} & \text{on } \Gamma_{\text{b}}, \\ Ae(\mathbf{p}_\Omega)\mathbf{n} = \mathbf{0} & \text{on } \Gamma \cup \left(\partial D \setminus (\overline{\Gamma_{\text{u}}} \cup \overline{\Gamma_{\text{b}}})\right), \\ Ae(\mathbf{p}_\Omega)\mathbf{n} = -2(\mathbf{u}_\Omega - \mathbf{u}_{\text{obs}}) & \text{on } \Gamma_{\text{u}}. \end{array} \right. \tag{5}$$

An outline of this calculation and a discussion about the nature of the adjoint state $\mathbf{p}_\Omega$ are provided in the supplementary material.

The expression (4) paves the way to a natural descent direction for $J_{\text{LS}}(\Omega)$:

$$\boldsymbol{\theta} = -v_\Omega \, \mathbf{n}. \tag{6}$$

2.4 Level-set representation

The magma chamber $\Omega \subset D$ is represented via the Level Set method, see e.g. (Osher & Fedkiw, 2006; Sethian, 1999), and the article (Allaire et al., 2004) about its introduction in shape and topology optimization. Briefly, Ω is described as the negative region of a scalar, "level set" function $\phi : D \to \mathbb{R}$.

$$\forall \mathbf{x} \in D, \quad \left\{ \begin{array}{ll} \phi(\mathbf{x}) < 0 & \text{if } \mathbf{x} \in \Omega, \\ \phi(\mathbf{x}) = 0 & \text{if } \mathbf{x} \in \Gamma, \\ \phi(\mathbf{x}) > 0 & \text{if } \mathbf{x} \in \Omega^c. \end{array} \right. \tag{7}$$

This idea is illustrated in a two-dimensional situation Fig. 2 (a).

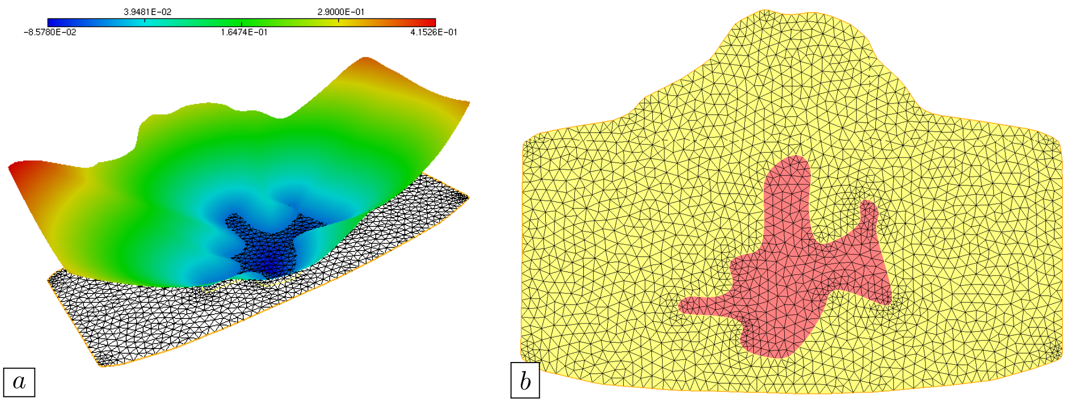

Figure 2. *(a) Graph of a level set function $\phi : D \to \mathbb{R}$ for the cavity Ω; (b) Meshed representation of Ω (in red), as a submesh of the total mesh of D.*

The evolution of a domain $\Omega(t)$ through a velocity field $\mathbf{V}(t,\mathbf{x})$, over a time period $(0,T)$ is conveniently captured in terms of an associated level set function $\phi(t,\cdot)$ (i.e. (7) holds for all $t \in [0,T]$); the latter indeed solves the following advection equation:

$$\forall t \in (0,T),\ \mathbf{x} \in D, \quad \frac{\partial \phi}{\partial t}(t,\mathbf{x}) + \mathbf{V}(t,\mathbf{x}) \cdot \nabla \phi(t,\mathbf{x}) = 0. \tag{8}$$

In this framework, dramatic changes of $\Omega(t)$ can be accounted for, including topological changes, i.e. merging of holes, or creation of holes.

In our application where $\Omega(t)$ is the sought solution of (2), the velocity field is the (negative) descent direction $\boldsymbol{\theta}$ in (6) and the time T stands for the descent step.

2.5 Numerical implementation

Our practical implementation leverages a recent variant of the level set method for shape optimization, introduced in (Allaire et al., 2014) – an open source implementation of which is proposed in (Dapogny & Feppon, 2023). The latter features an additional step at each optimization iteration $n = 0, \ldots$, during which remeshing algorithms are used to create a meshed description of Ω^n, as a submesh of the computational domain D, see Fig. 2

Our numerical workflow is sketched in Alg. 1. The associated code, named `magmaOpt`, is freely available online in (Perrot, 2024), and comprehensive information about its use is provided in the supplementary material.

Algorithm 1 Shape optimization algorithm for the reconstruction of a magma chamber.

Initialization: Initial shape $\Omega^0 \subset D$, mesh $\mathcal{T}^0$ of D a submesh $\mathcal{T}^0_{\text{cav}}$ of which accounts for Ω^0.
for $n = 0, ...,$ until stop criterion is met **do**
1. Calculate a level set function $\phi^n : D \to \mathbb{R}$ for Ω^n on $\mathcal{T}^n$.
2. Calculate the state $\mathbf{u}_{\Omega^n}$ and adjoint state $\mathbf{p}_{\Omega^n}$ on $\mathcal{T}^n_{\text{cav}}$.
3. Calculate a descent direction $\boldsymbol{\theta}^n$ for J_{LS}, from Ω^n on $\mathcal{T}^n$.
4. Update the level set function by solving the advection equation (8) on $\mathcal{T}^n$.
5. Create a new mesh $\mathcal{T}^{n+1}$ of D in which Ω^{n+1} exists as a submesh.

end for
return Optimized shape $\Omega^n \subset D$ of the cavity.

The initial geometry is created thanks to the open-source software `Gmsh` (Geuzaine et al., 2009). At each iteration n, the computational domain D is discretized by a mesh $\mathcal{T}^n$ which encloses a discretization of the actual shape Ω^n of the magma chamber as a submesh $\mathcal{T}^n_{\text{cav}}$. The state and adjoint systems (1) and (5) for $\mathbf{u}_{\Omega^n}$ and $\mathbf{p}_{\Omega^n}$ are solved on this mesh by the open-source Finite Element library `FreeFem` (Hecht, 2012). A descent direction $\boldsymbol{\theta}^n$ is then obtained by (6), and a level set function ϕ^n for the next iterate Ω^{n+1} is obtained by solving (8) thanks to the open-source library `Advect` (Bui et al., 2012). The optimization procedure relies on the null-space algorithm (Feppon, Allaire, & Dapogny, 2020), which handles efficiently infinite-dimensional problems as well as bounds, equality and inequality constraints.

3 Results

3.1 Validation on synthetic data

TP: [Paragraph below ok] To validate the proposed method, cross-validation tests were peformed. Synthetic observation data was generated from a known source using the analytical solution provided by McTigue (1987), who derived the expression of the surface displacement field caused by a uniformly pressurized spherical cavity embedded in an isotropic and homogeneous elastic medium. `magmaOpt` was initialized with various arbitrary first guesses for the source shape and position. Other model parameters (elastic constants, internal pressures) were fixed for both synthetic data generation and shape optimization.

Behaviors to mention

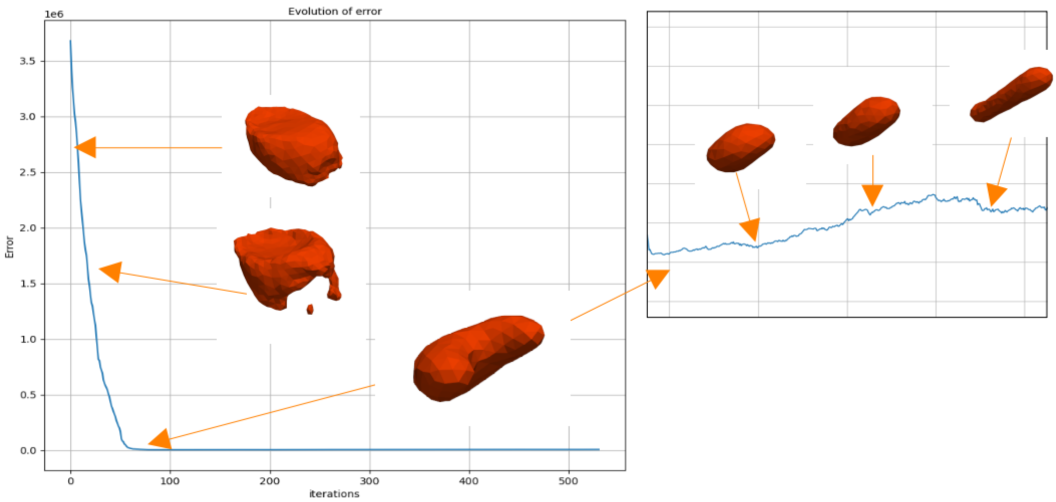

Figure 3. $^{TP:}$ [CHANGE the figure] . Evolution of error and succesive shapes taken by the magma source during an optimization loop. The initial guess is a flat ellipsoid of semi-axes $r_x = 2\text{km}, r_y = 3\text{km}, r_z = 1\text{km}$
centred on the true spherical source. The minimum is reached at iteration 82.

$^{TP:}$ [DISCUSS WHAT TO PUT HERE]

3.2 Test case : magma recharge at Svartsengi, 2022

$^{TP:}$ [Intro OK ?] The shape of a magma chamber was inferred from the ground inflation observed at Svartsengi, South-West of Iceland, during the period from 21 April to 14 June 2022. This event was one of five inflation episodes that preceded dike breaches at the Sundhnúkur crater row, resulting in the partial destruction of Grindavík (Sigmundsson et al., 2024).

The observational data utilized consisted of unwrapped InSAR line-of-sight (LOS) displacement maps of the area, obtained from Cosmo SkyMed satellite and available at Parks et al. (2024). After uniform downsampling and mesh reprojection, both ascending A32 and descending D132 tracks were employed. A slight modification of the least-square function was needed because of the peculiar geometry of InSAR data :

$$J_{\text{LS}}^{los}(\Omega) := \int_{\Gamma_u} \sum_{i \in \text{tck}} \alpha_i (\mathbf{u}_\Omega \cdot \mathbf{l}_i - d_i^{\text{obs}})^2 \, \mathrm{d}s \tag{9}$$

where $\text{tck} = A125, D132$ is the list of used tracks. For each track i, α_i is its weight (here we choosed $\forall i, \alpha_i = 1$), $\mathbf{l}_i$ is the LOS unit vector of the track (giving the look direction of the satellite to project 3D displacment into LOS geometry), and d_i^{obs} is the observed LOS displacement.

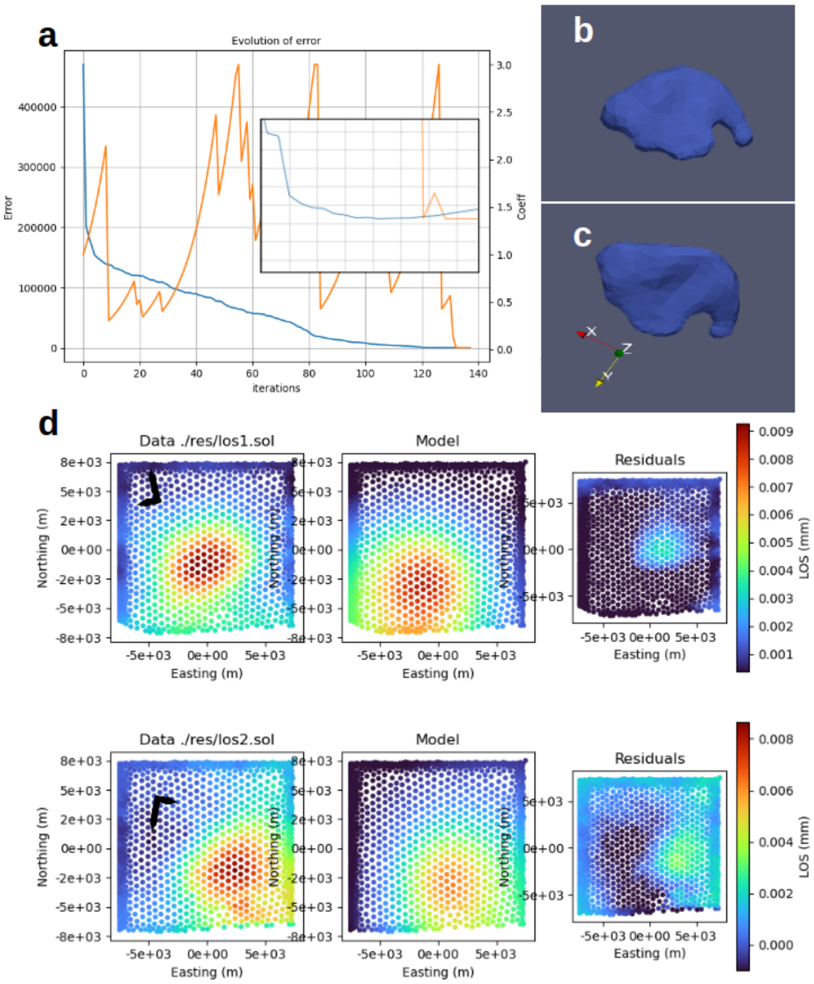

Figure 4. a) Convergence plot with embedded zoom. The blue line is the error and the orange line is the evolution of τ. Minima are reached at iteration 128. b,c) Side and top view of the source Γ_s minimizing J. d) Data, model and residuals of the LOS displacements at iteration 128 for the two InSAR tracks A32 (top) and D132 (bottom). Black arrows are heading and looking directions, coordinates are ISN16 (Valsson, 2019) shifted to a local origin $(2529373E, 179745N)$.

The results shown in figure 4 are encouraging: after providing an initial guess located at the center of inflation at depth for a sphere of radius RR, the algorithm is able to iteratively change the shape and depth of the magma domain to finally result in a sill-like flattened spheroid whose centroid is located at DD depth. This is consistent with the presumed depth found in the supporting information of (Sigmundsson et al., 2024), which performs an analytical model-based inversion. Although the pressure must be fixed, as explained in 1.1, the result can be used to compare the final shape of the magmatic intrusion and give a richer insight into it. Here we see interesting features, such as an increasing thickness on the north side, that can't be traced by any other method. The algorithm produces features that we consider to be artifacts, probably due to mesh refinement problems, such as small holes or horn-shaped features.

^{TP}: [Above more detailed characterization of the results is needed as well as comparison with the analytical results]

4 Discussion

^{TP}: [Discussio complete enough ? Should have more ref ? Might change as well]

This work paves the way for a new class of methods that tackle an unknown geometry of the magmatic domains, thus giving the possibility to explore irregular shapes that are more likely to exist compared to any other usually assumed regular shapes. However, even if the first results presented are promising, many questions remain to be answered.

First of all, the internal pressure of the chamber ΔP must be specified prior to the shape optimization, while for conventional parametric inversions, the pressure is a model parameter optimized alongside the position and shape parameters. To adress this limitation, a potential approach would involve two stages in the optimization. A conventional inversion of a parametric model would be run first, giving a pressure and a first educated guess for the position for Ω. Then a more realistic shape could be sought with a shape optimization taking the output of the parametric inversion as an initial guess. Finally, the parametric optimization would be run again using the new shape as input but optimizing only ΔP. This two final steps could be then run succesively until convergence of Ω and ΔP. While this two-stage procedure is theoretically sound, further investigation and implementation are necessary to determine its practical feasibility.

As showed in part 3.1, the produced design depend strongly on the prior knowledge, namely the intial guess here. Adding constraints is a way to put more knowledge in the inversion, and get more repeatable results. For example, the volume of the source could be constrained to stay within bounds or even to match a certain value. The implemented shape optimization is certainly able to handle constraints as described by Allaire et al. (2021), and is in practice almost always constrained in other application. The physical meaning of the best shape might benefit from a more constrained problem.

To better understand the influence of data partitioning and variablitiy, additional tests should be run with synthetic data. We can think of tests such as masking part of the surface displacement field, introducing noise and parasitic signals, reducing the number of data points, as is often the case in reality with areas of volcanic systems lacking data coverage (glacier, river, lava, forest) and subjected to perturbations such as atmospheric distorsions.

It is also important to mention that the behaviour of the algorithm is influenced by numerous parameters of varying importance, starting from the discretization length (element size) or the domain extent, to the limits of the step size τ, the regularization length, or the number of iterations allowed by the line search. A systematic study of each of these parameters would be beneficial in assessing the quality of the shape inferred.

5 Conclusion

^{TP}: [Conclusion OK ? Check about the role of a conclusion]

We have shown here, to some extent, the relevance of applying shape optimization to identify the likely shapes taken by a magma chamber using as sole information the measured surface displacement field. ^{TP}:The set of source shapes found with the tests on real was representative of the diversity of behavior to be expected from the algorithm and underlined the intrinsic non-unicity of the solution to the problem, but demonstrated coherence in the results. [TO modify depending on the results] The test on real data from Svarstengi 2022 inflation showed a concrete case of how the method could be used after being more mature while displaying a credible solution.

This work was intended as an opening to a new method of interest to the field of volcanology rather than a complete solution, and we hilighted the main limitation. Nevertheless, the code `magmaOpt` provided with this paper can serve as a basis for future modifications and improvements of the method.

The perspectives are many. Besides necessary modifications, such as constraining the problem with more prior knowledge or characterizing the behavior of the algorithm precisely, more sophisticated models could be involved for the inversion. The versatile nature of the finite element method allows the addition of external loads (e.g tectonic stresses, tidal loads, glacier weights), complex topographic geometries and advanced mechanical behavior of the crust (e.g plasticity, viscoelasticity, poroelasticity). By addressing these limitations and extending this approach, the accuracy and reliability of volcanic source inference can be improved. Ultimately, future developments may enable better monitoring of volcanic activity, prediction of eruptions, and provide critical support for hazard mitigation strategies.

Open Research Section

This section MUST contain a statement that describes where the data supporting the conclusions can be obtained. Data cannot be listed as "Available from authors" or stored solely in supporting information. Citations to archived data should be included in your reference list. Wiley will publish it as a separate section on the paper's page. Examples and complete information are here: https://www.agu.org/Publish with AGU/Publish/Author Resources/Data for Authors

As Applicable – Inclusion in Global Research Statement

The Authorship: Inclusion in Global Research policy aims to promote greater equity and transparency in research collaborations. AGU Publications encourage research collaborations between regions, countries, and communities and expect authors to include their local collaborators as co-authors when they meet the AGU Publications authorship criteria (described here: https://www.agu.org/publications/authors/policies#authorship). Those who do not meet the criteria should be included in the Acknowledgement section. We encourage researchers to consider recommendations from The TRUST CODE - A Global Code of Conduct for Equitable Research Partnerships (https://www.globalcodeofconduct.org/) when conducting and reporting their research, as applicable, and encourage authors to include a disclosure statement pertaining to the ethical and scientific considerations of their research collaborations in an "Inclusion in Global Research Statement' as a standalone section in the manuscript following the Conclusions section. This can include disclosure of permits, authorizations, permissions and/or any formal agreements with local communities or other authorities, additional acknowledgements of local help received, and/or description of end-users of the research. You can learn more about the policy in this editorial. Example statements can be found in the following published papers: Holt et al. (https://agupubs.onlinelibrary.wiley.com/doi/full/10.1029/2022JG007188), Sánchez-Gutiérrez et al. (https://agupubs.onlinelibrary.wiley.com/doi/abs/10.1029/2023JG007554), Tully et al. (https://agupubs.onlinelibrary.wiley.com/doi/epdf/10.1029/2022JG007128) Please note that these statements are titled as "Global Research Collaboration Statements" from a previous pilot requirement in JGR Biogeosciences. The pilot has ended and statements should now be titled "Inclusion in Global Research Statement".

Acknowledgments

Enter acknowledgments here. This section is to acknowledge funding, thank colleagues, enter any secondary affiliations, and so on.

References

Allaire, G. (2006). *Conception Optimale de Structures* (Vol. 58). Springer Berlin Heidelberg. doi: 10.1007/978-3-540-36856-4

Allaire, G., Dapogny, C., & Frey, P. (2014). Shape optimization with a level set based mesh evolution method. *Computer Methods in Applied Mechanics and Engineering*, *282*, 22–53.

Allaire, G., Dapogny, C., & Jouve, F. (2021). Chapter 1 - Shape and Topology Optimization. In A. Bonito & R. H. Nochetto (Eds.), *Geometric Partial Differential Equations - Part II* (Vol. 22, pp. 1–132). Elsevier. doi: 10.1016/bs.hna.2020.10.004

Allaire, G., Jouve, F., & Toader, A.-M. (2004). Structural optimization using sensitivity analysis and a level-set method. *Journal of computational physics*, *194*(1), 363–393.

Bagnardi, M., & Hooper, A. (2018, July). Inversion of Surface Deformation Data for Rapid Estimates of Source Parameters and Uncertainties: A Bayesian Approach. *Geochemistry, Geophysics, Geosystems*, *19*(7), 2194–2211. doi: 10.1029/2018GC007585

Bendsoe, M. P., & Sigmund, O. (2004). Topology Optimization by Distribution of Isotropic Material. In M. P. Bendsoe & O. Sigmund (Eds.), *Topology Optimization: Theory, Methods, and Applications* (pp. 1–69). Berlin, Heidelberg: Springer. doi: 10.1007/978-3-662-05086-6_1

Bui, C., Dapogny, C., & Frey, P. (2012). An accurate anisotropic adaptation method for solving the level set advection equation. *International Journal for Numerical Methods in Fluids*, *70*(7), 899–922.

Cea, J. (1986). Conception Optimale Ou Identification de Formes, Calcul Rapide de La Dérivée Directionnelle de La Fonction Coût. *ESAIM: Modélisation mathématique et analyse numérique*, *20*(3), 371–402.

Cervelli, P., Murray, M. H., Segall, P., Aoki, Y., & Kato, T. (2001). Estimating Source Parameters from Deformation Data, with an Application to the March 1997 Earthquake Swarm off the Izu Peninsula, Japan. *Journal of Geophysical Research: Solid Earth*, *106*(B6), 11217–11237. doi: 10.1029/2000JB900399

Charco, M., & Galán del Sastre, P. (2014, March). Efficient Inversion of Three-Dimensional Finite Element Models of Volcano Deformation. *Geophysical Journal International*, *196*(3), 1441–1454. doi: 10.1093/gji/ggt490

Dapogny, C., & Feppon, F. (2023, October). Shape Optimization Using a Level Set Based Mesh Evolution Method: An Overview and Tutorial. *Comptes Rendus. Mathématique*, *361*(G8), 1267–1332. doi: 10.5802/crmath.498

Dzurisin, D. (2007). *Volcano Deformation: Geodetic Monitoring Techniques*. Berlin ; New York : Chichester, UK: Springer ; Praxis.

Feppon, F., Allaire, G., & Dapogny, C. (2020). Null space gradient flows for constrained optimization with applications to shape optimization. *ESAIM: Control, Optimisation and Calculus of Variations*, *26*, 90. doi: 10.1051/cocv/2020015

Feppon, F., Allaire, G., Dapogny, C., & Jolivet, P. (2020, September). Topology Optimization of Thermal Fluid–Structure Systems Using Body-Fitted Meshes and Parallel Computing. *Journal of Computational Physics*, *417*, 109574. doi: 10.1016/j.jcp.2020.109574

Frei, W. (2015, December). *Designing New Structures with Shape Optimization.* COMSOL.

Geuzaine, C., Remacle, J.-F., & Dular, P. (2009). Gmsh: A Three-Dimensional Finite Element Mesh Generator. *International Journal for Numerical Methods in Engineering*, *79*(11), 1309–1331.

Hecht, F. (2012). New Development in FreeFem++. *Journal of Numerical Mathematics*, *20*(3-4), 251–265.

Henrot, A., & Pierre, M. (2018). *Shape Variation and Optimization.* EMS Tracts in Mathematics Vol. 28.

Hickey, J., & Gottsmann, J. (2014, June). Benchmarking and Developing Numerical Finite Element Models of Volcanic Deformation. *Journal of Volcanology and Geothermal Research*, *280*, 126–130. doi: 10.1016/j.jvolgeores.2014.05.011

Le Quilliec, G. (2014). Topology Optimization Procedure TOPOPTIM and Other Various Developments Made with Cast3M. doi: 10.13140/2.1.2718.3682

Lucchini, F., Torchio, R., Cirimele, V., Alotto, P., & Bettini, P. (2022). Topology optimization for electromagnetics: A survey. *IEEE Access*, *10*, 98593–98611.

McTigue, D. F. (1987, November). Elastic Stress and Deformation near a Finite Spherical Magma Body: Resolution of the Point Source Paradox. *Journal of Geophysical Research: Solid Earth*, *92*(B12), 12931–12940. doi: 10.1029/JB092iB12p12931

Mogi, K. (1958). Relations between the Eruptions of Various Volcanoes and the Deformations of the Ground Surfaces around Them. *Earthq Res Inst*, *36*, 99–134.

Murat, F., & Simon, J. (1976). Sur le contrôle par un domaine géométrique. *Pré-publication du Laboratoire d'Analyse Numérique,(76015).*

Osher, S., & Fedkiw, R. (2006). *Level set methods and dynamic implicit surfaces* (Vol. 153). Springer Science & Business Media.

Parks, M., Drouin, V., Geirsson, H., Hooper, A., Hreinsdóttir, S., Ófeigsson, B., ... Tolpekin, V. (2024, January). Data and Geodetic Modelling Results for Science Article "Fracturing and Tectonic Stress Drives Ultra-Rapid Magma Flow into Dikes".

Perrot, T. (2024). *\texttt magmaOpt.*

Plessix, R.-E. (2006). A review of the adjoint-state method for computing the gradient of a functional with geophysical applications. *Geophysical Journal International*, *167*(2), 495–503.

Sethian, J. A. (1999). *Level set methods and fast marching methods: Evolving interfaces in computational geometry, fluid mechanics, computer vision, and materials science* (Vol. 3). Cambridge university press.

Sigmund, O. (2001, April). A 99 Line Topology Optimization Code Written in Matlab. *Structural and Multidisciplinary Optimization*, *21*(2), 120–127. doi: 10.1007/s001580050176

Sigmund, O., & Maute, K. (2013, December). Topology Optimization Approaches: A Comparative Review. *Structural and Multidisciplinary Optimization*, *48*(6), 1031–1055. doi: 10.1007/s00158-013-0978-6

Sigmundsson, F., Parks, M., Geirsson, H., Hooper, A., Drouin, V., Vogfjörd, K. S., ... Barsotti, S. (2024, February). Fracturing and Tectonic Stress Drives Ultrarapid Magma Flow into Dikes. *Science*, eadn2838. doi: 10.1126/science.adn2838

Slavov, S., & Konsulova-Bakalova, M. (2019, January). Optimizing Weight of Housing Elements of Two-stage Reducer by Using the Topology Management Optimization Capabilities Integrated in SOLIDWORKS: A Case Study. *Machines*, *7*(1), 9. doi: 10.3390/machines7010009

Taylor, N. C., Johnson, J. H., & Herd, R. A. (2021, November). Making the Most of the Mogi Model: Size Matters. *Journal of Volcanology and Geothermal Research*, *419*, 107380. doi: 10.1016/j.jvolgeores.2021.107380

Trasatti, E. (2022, July). Volcanic and Seismic Source Modeling: An Open Tool for Geodetic Data Modeling. *Frontiers in Earth Science*, *10*. doi: 10.3389/feart.2022.917222

Valssson, G. Þ. (2019, March). *ISN2016 - Tækniskýrsla* (Tech. Rep.). Íslands: Landmælingar.

Velez, M. L., Euillades, P., Caselli, A., Blanco, M., & Díaz, J. M. (2011, April). Deformation of Copahue Volcano: Inversion of InSAR Data Using a Genetic Algorithm. *Journal of Volcanology and Geothermal Research*, *202*(1), 117–126. doi: 10.1016/j.jvolgeores.2011.01.012

Yang, X.-M., Davis, P. M., & Dieterich, J. H. (1988). Deformation from Inflation of a Dipping Finite Prolate Spheroid in an Elastic Half-Space as a Model for Volcanic Stressing. *Journal of Geophysical Research: Solid Earth*, *93*(B5), 4249–4257. doi: 10.1029/JB093iB05p04249